RAA 2021 Vol. **21** No. **2**, 35(7pp) doi: 10.1088/1674-4527/21/2/35

http://www.raa-journal.org *http://iopscience.iop.org/raa*

***R**esearch in*
***A**stronomy and*
***A**strophysics*

Can we constrain the evolution of HI bias using configuration entropy?

Biswajit Das and Biswajit Pandey

Department of Physics, Visva-Bharati University, Santiniketan, Birbhum, 731235, India; *bishoophy@gmail.com, biswap@visva-bharati.ac.in*

Received 2020 April 11; accepted 2020 June 18

Abstract We study the evolution of the configuration entropy of HI distribution in the post-reionization era assuming different time evolution of HI bias. We describe time evolution of linear bias of HI distribution using a simple form $b(a) = b_0 a^n$ with different index n. The derivative of the configuration entropy rate is known to exhibit a peak at the scale factor corresponding to the Λ-matter equality in the unbiased ΛCDM model. We show that in the ΛCDM model with time-dependent linear bias, the peak shifts to smaller scale factors for negative values of n. This is related to the fact that the growth of structures in the HI density field can significantly slow down even before the onset of Λ domination in the presence of a strong time evolution of the HI bias. We find that the shift is linearly related to the index n. We obtain the best fit relation between these two parameters and propose that identifying the location of this peak from observations would allow us to constrain the time evolution of HI bias within the framework of the ΛCDM model.

Key words: methods: analytical — cosmology: theory — large scale structure of the universe

1 INTRODUCTION

Our knowledge about the present day galaxy distribution in the nearby Universe has been revolutionized by modern galaxy surveys (SDSS, York et al. 2000; 2dFGRS, Colless et al. 2001; 2MRS, Huchra et al. 2012) carried out over the last few decades. Many cosmological observations suggest that most of the mass in the Universe is in the form of an unseen dark matter which is yet to be directly detected by observations. The galaxies are known to be a biased tracer of the underlying dark matter distribution. On large scales, it is believed that the fluctuations in the galaxy distribution and the dark matter distribution are linearly related by a bias parameter (Kaiser 1984; Dekel & Rees 1987). The linear bias parameter is known to be scale-independent on large scales (Mann et al. 1998) but is expected to evolve with time (Fry 1996; Tegmark & Peebles 1998). The time evolution of the linear bias parameter determines the evolution of the large scale distribution of the tracer relative to the underlying mass distribution. However, the galaxies have not always been in place. They are the product of the non-linear evolution of the cosmic density field. Thanks to the improvement of computing power and algorithms, modern day N-body simulations (Springel et al. 2005; Vogelsberger et al. 2014) can give us a clear idea about the emergence of structures through non-linear evolution. In fact, the understanding of the process of structure formation has become so good that it has become a standard tool for testing cosmological models.

Early measurements of the two point correlation function for galaxies and galaxy clusters did not match, indicating that both cannot be unbiased tracers of the underlying matter distribution (Kaiser 1984). Various statistical tools are applied to measure the linear bias parameter from observations. One can employ the two-point correlation function and power spectrum to determine the linear bias parameter (Norberg et al. 2001; Tegmark et al. 2004; Zehavi et al. 2011). The redshift space distortions of the two-point correlation function and power spectrum (Kaiser 1987; Hamilton 1992) can be also utilized to measure the linear bias parameter (Hawkins et al. 2003; Tegmark et al. 2004). The other alternatives which have been successfully implemented to compute the linear bias parameter are the three-point correlation function and bispectrum (Feldman et al. 2001; Verde et al. 2002; Gaztañaga et al. 2005), filamentarity (Pandey & Bharadwaj 2007) and information entropy (Pandey 2017a). It has been shown by Pandey (2017a) that measurement of bias using information entropy requires only $O(N)$ operations as compared to $O(N^2)$ or at least $O(N \log N)$ operations required by the two-point correlation function and the power spectrum.

Galaxies do not exist at high redshift whereas neutral hydrogen (HI) is present throughout the history of the Universe since its formation after the recombination at $z \sim 1100$. The redshifted 21 cm line from neutral hydrogen would reveal a wealth of information about the formation and evolution of structures in the Universe. A number of surveys (HIPASS, Zwaan et al. 2005; ALFALFA, Martin et al. 2012) have been designed to map the HI content of galaxies in the nearby Universe. A significant effort has been also directed to detect the redshifted 21 cm signal by relying on different ongoing and upcoming radio interferometric facilities (GMRT, Paciga et al. 2013; LOFAR, van Haarlem et al. 2013; MWA Bowman et al. 2013; SKA, Mellema et al. 2013). The redshifted 21 cm line can be used as a promising probe of the large scale structures over a wide redshift range (Bharadwaj et al. 2001; Bharadwaj & Sethi 2001). Knowledge about the HI bias and its time evolution is also important in understanding the uncertainties associated with the measured intensity fluctuation power spectrum. Several studies have been carried out to measure the HI bias (Martin et al. 2012; Masui et al. 2013; Switzer et al. 2013) at low redshifts ($z < 1$) but presently the evolution of HI bias with redshift is not known. Some theoretical and observational constraints on the evolution of HI bias over the redshift range $0 - 3.5$ have been discussed in Padmanabhan et al. (2015) and references therein.

Most of the HI resides in the intergalactic medium during the epoch of reionization. The HI distribution deviates from the dark matter distribution due to the non-linear growth of ionized hydrogen (HII) bubbles and formation of early galaxies during this epoch. The HI distribution cannot be treated as a tracer of the underlying matter density field during the epoch of reionization. However, most of the HI settles in halos after reionization and the HI distribution can be treated as a reliable tracer of the total mass distribution in the post-reionization era. The HI bias in the post-reionization era has been studied in some works (Bagla et al. 2010; Sarkar et al. 2016) by populating HI in dark matter halos from N-body simulations.

Recently, it has been suggested that measurement of the configuration entropy (Pandey 2017b, 2019) of the mass distribution in the Universe can be utilized to test the different cosmological models (Das & Pandey 2019), determine the mass density parameter and cosmological constant (Pandey & Das 2019) and constrain the dark energy equation of state parameters (Das & Pandey 2020). In the present work, we propose a theoretical framework based on the study of configuration entropy which may allow us to probe the evolution of HI bias in the post-reionization era from future redshifted 21 cm observations.

2 THEORY

2.1 Evolution of Configuration Entropy

We consider the HI distribution in the post-reionization era which can be treated as a biased tracer of the underlying dark matter distribution. We are interested in studying the time evolution of the linear bias of HI distribution using configuration entropy. Let us consider a large comoving volume V of the Universe and divide it into sub-volumes dV. Let the density of HI in each of these sub-volumes at time t be $\rho_{\rm HI}(\boldsymbol{x}, t)$ where $\boldsymbol{x}$ is the comoving coordinate of the sub-volume defined with respect to an arbitrary origin. The configuration entropy of the HI density field can be defined as (Pandey 2017b),

$$S_c(t) = -\int \rho_{\rm HI}(\boldsymbol{x}, t) \log \rho_{\rm HI}(\boldsymbol{x}, t)\, dV. \tag{1}$$

The definition of configuration entropy is motivated from the definition of information entropy (Shannon 1948).

The mass distribution of the Universe is often treated as an ideal fluid to a good approximation. The continuity equation of this fluid in an expanding Universe can be written as,

$$\frac{\partial \rho_{\rm HI}}{\partial t} + 3\frac{\dot{a}}{a}\rho_{\rm HI} + \frac{1}{a}\nabla \cdot (\rho_{\rm HI}\boldsymbol{v_{\rm HI}}) = 0. \tag{2}$$

In Equation (2), a is the cosmological scale factor and $\boldsymbol{v_{\rm HI}}$ is the peculiar velocity of the HI mass element. We can combine Equation (1) and Equation (2) to get,

$$\frac{dS_c(t)}{dt} + 3\frac{\dot{a}}{a}S_c(t) - \frac{1}{a}\int \rho_{\rm HI}(3\dot{a} + \nabla \cdot \boldsymbol{v_{\rm HI}})\, dV = 0. \tag{3}$$

We rewrite Equation (3) as,

$$\begin{aligned}\frac{dS_c(a)}{da}\dot{a} + 3\frac{\dot{a}}{a}S_c(a) - 3\frac{\dot{a}}{a}\int \rho_{\rm HI}(\boldsymbol{x}, a)\, dV \\ - \frac{1}{a}\int \rho_{\rm HI}(\boldsymbol{x}, a)\nabla \cdot \boldsymbol{v_{\rm HI}}\, dV = 0,\end{aligned} \tag{4}$$

where the variable of differentiation has been changed from t to a. Here $\int \rho_{\rm HI}(\boldsymbol{x}, a)\, dV = M_{\rm HI}$ is the total mass of HI contained inside the comoving volume V. The density of HI at comoving location $\boldsymbol{x}$ can be expressed as $\rho_{\rm HI}(\boldsymbol{x}, a) = \bar{\rho}_{\rm HI}(1 + \delta_{\rm HI}(\boldsymbol{x}, a))$, where $\delta_{\rm HI}(\boldsymbol{x}, a)$ is the density contrast at location $\boldsymbol{x}$ and $\bar{\rho}_{\rm HI} = \frac{M_{\rm HI}}{V}$ is the average density of HI. In linear perturbation theory, one can write $\delta_m(\boldsymbol{x}, a) = D(a)\delta_m(\boldsymbol{x})$ and $\nabla \cdot \boldsymbol{v_{\rm HI}} = -a\frac{\partial \delta_{\rm HI}(\boldsymbol{x}, a)}{\partial t}$. Here, $D(a)$ is the growing mode and $\delta_m(\boldsymbol{x})$ is the initial mass density perturbation at location $\boldsymbol{x}$. We simplify Equation (4) applying these relations to get,

$$\begin{aligned}\frac{dS_c(a)}{da}\dot{a} + 3\frac{\dot{a}}{a}(S_c(a) - M_{\rm HI}) - \frac{\bar{\rho}_{\rm HI}}{a}\int \nabla \cdot \boldsymbol{v_{\rm HI}}\, dV \\ - \frac{\bar{\rho}_{\rm HI}}{a}\int \delta_{\rm HI}(\boldsymbol{x}, a)\nabla \cdot \boldsymbol{v_{\rm HI}}\, dV = 0.\end{aligned} \tag{5}$$

In the linear bias assumption,

$$\delta_{\rm HI}(\boldsymbol{x}, a) = b(a)\delta_m(\boldsymbol{x}, a), \tag{6}$$

where $b(a)$ is the scale-independent linear bias parameter and $\delta_{\rm HI}(\boldsymbol{x}, a)$ and $\delta_m(\boldsymbol{x}, a)$ are the density contrast corresponding to HI and the underlying mass density field respectively. So,

$$\nabla \cdot \boldsymbol{v}_{\rm HI} = -a\dot{a}\left[D(a)\frac{db(a)}{da} + b(a)\frac{dD(a)}{da}\right]\delta_m(\boldsymbol{x}). \tag{7}$$

We combine Equation (7) and Equation (5) and simplify to get,

$$\begin{aligned}\frac{dS_c(a)}{da} + \frac{3}{a}(S_c(a) - M_{\rm HI}) \\ + \bar{\rho}_{\rm HI}B(a)\int \delta_m^2(\boldsymbol{x})\, dV = 0.\end{aligned} \tag{8}$$

Here, $B(a) = b(a)D(a)\left[D(a)\frac{db(a)}{da} + b(a)\frac{f(a)D(a)}{a}\right]$ where $f(a) = \frac{a}{D(a)}\frac{dD(a)}{da}$ is the dimensionless linear growth rate.

This equation governs the evolution of configuration entropy of the HI distribution in the presence of time evolution of HI bias. One can integrate Equation (8) to get

$$\begin{aligned}\frac{S_c(a)}{S_c(a_i)} = \frac{M_{\rm HI}}{S_c(a_i)} + \left[1 - \frac{M_{\rm HI}}{S_c(a_i)}\right]\left(\frac{a_i}{a}\right)^3 \\ - \left(\frac{\bar{\rho}_{\rm HI}\int \delta_m^2(\boldsymbol{x})\, dV}{S_c(a_i)a^3}\right)\int_{a_i}^{a} da' a'^3 B(a').\end{aligned} \tag{9}$$

Here a_i is some initial scale factor and $S_c(a_i)$ is the initial configuration entropy. In our analysis, we have chosen $a_i = 0.05$.

We find the evolution of the ratio of configuration entropy to its initial value by numerically calculating the integral in the third term for different time evolutions of bias and substituting back into Equation (9). We set the product $\bar{\rho}_{\rm HI}\int \delta_m^2(\boldsymbol{x})\, dV = 1$ for simplicity. The choices of $S_c(a_i)$ and $M_{\rm HI}$ are arbitrary and in no way depend on the cosmological model concerned. Selecting $S_c(a_i) > M_{\rm HI}$ or $S_c(a_i) < M_{\rm HI}$ causes a sudden growth or decay in $\frac{S_c(a)}{S_c(a_i)}$ near the initial scale factor a_i, respectively. We have chosen $S_c(a_i) = M_{\rm HI}$ in our analysis to ignore these transients caused by the initial conditions. The integral in the third term of Equation (9) involves evolution of growing mode, time dependent bias and their derivatives. We describe these in detail in the next two subsections.

2.2 Growth Rate of Density Perturbations

Cosmic microwave background radiation (CMBR) observations suggest that the Universe was highly isotropic at $z \sim 1100$, but the present day Universe is neither homogeneous nor isotropic on small scales. We find galaxies and clusters of galaxies where huge mass is accumulated over a small region whereas there are large empty regions or voids with very little amount of mass. Linear perturbation theory provides a theoretical framework to understand the growth of structures from tiny fluctuations seeded in a homogeneous and isotropic distribution in the early Universe. In the currently accepted paradigm, gravitational instability is the primary mechanism behind the formation of structures in the Universe. CMBR observations indicate that inhomogenities of very small magnitude were present in the matter distribution at the time of recombination. These tiny inhomogeneities get amplified by gravitational instability over time. When the density contrast is much smaller than 1, its evolution can be described by the following differential equation,

$$\begin{aligned}\frac{\partial^2\delta_m(\boldsymbol{x}, t)}{\partial t^2} + 2H(a)\frac{\partial\delta_m(\boldsymbol{x}, t)}{\partial t} \\ - \frac{3}{2}\Omega_{m0}H_0^2\frac{1}{a^3}\delta_m(\boldsymbol{x}, t) = 0.\end{aligned} \tag{10}$$

Here we have considered perturbation to only matter component. Ω_{m0} and H_0 are the present value of density parameter for matter and Hubble parameter, respectively. This equation governs the growth of density perturbation in the underlying matter distribution. The equation has a growing mode solution in the form $\delta_m(\boldsymbol{x}, t) = D(t)\delta_m(\boldsymbol{x})$. The growing mode solution can be expressed as (Peebles 1980)

$$D(a) = \frac{5}{2}\Omega_{m0}X^{\frac{1}{2}}(a)\int_0^a \frac{da'}{a'^3X^{\frac{3}{2}}(a')}, \tag{11}$$

where $X(a) = \frac{H^2(a)}{H_0^2} = [\Omega_{m0}a^{-3} + \Omega_{\Lambda 0}]$. Here $\Omega_{\Lambda 0}$ is the present value of the density parameter corresponding to the cosmological constant.

The dimensionless linear growth rate $f(a) = \frac{d\log D(a)}{d\log a}$ in a Universe with no curvature can be approximated as (Lahav et al. 1991)

$$\begin{aligned}f(a) = \Omega_m(a)^{0.6} \\ + \frac{1}{70}\left[1 - \frac{1}{2}\Omega_m(a)(1 + \Omega_m(a))\right].\end{aligned} \tag{12}$$

Here $\Omega_m(a) = \frac{\Omega_{m0}a^{-3}}{X(a)}$. We have used $\Omega_{m0} = 0.3$ and $\Omega_{\Lambda 0} = 0.7$ throughout the present work.

2.3 Evolution of HI Bias

The time evolution of the HI bias parameter is expected to affect the time evolution of the configuration entropy of the HI density field. We consider a simple power law of the form $b(a) = b_0a^n$ with different possible values of n. The functional form is motivated by Bagla et al. (2010) where $b(z) \propto (1 + z)^{0.5}$ was reported to give

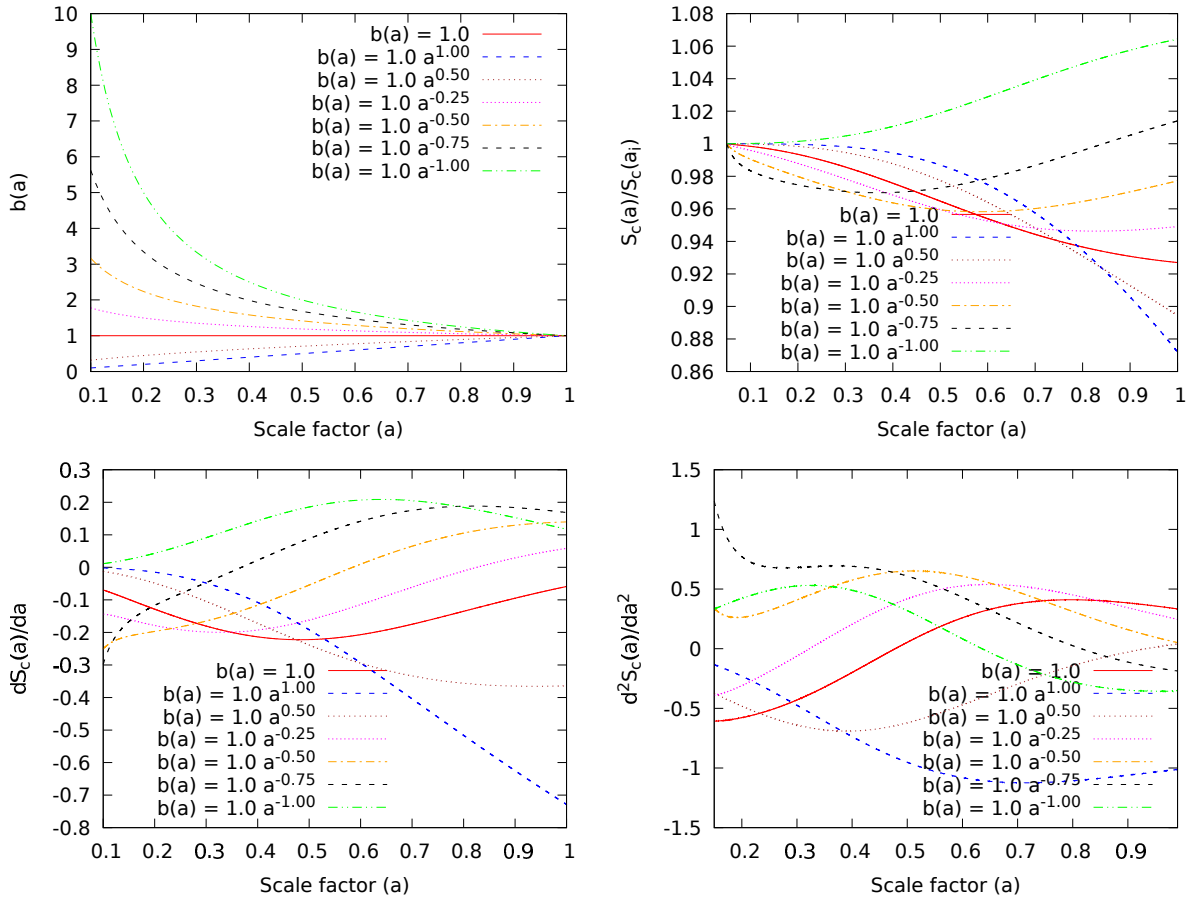

Fig. 1 The *top left panel* in the figure displays the evolution of bias with scale factor for different models. The *top right panel* plots the evolution of $S_c(a)/S_c(a_i)$ with scale factor for different evolutions of bias within the ΛCDM model. The *bottom left* and *right panels* respectively depict the evolution of $dS_c(a)/da$ and $d^2S_c(a)/da^2$ with scale factor for the same models. The results for the unbiased case $b = 1$ are also shown in each panel for comparison.

a reasonably good description of the evolution of HI bias in the simulated HI distributions from the N-body simulations. We consider the following values of n in our analysis: $n = -1, -0.75, -0.5, -0.25, 0.5, 1$. We also incorporate the unbiased ΛCDM model in this framework by putting $b(a) = b_0$. We set $b_0 = 1$ in all the models considered here.

3 RESULTS AND CONCLUSIONS

We display the evolution of the HI bias with scale factor for different values of n in the top left panel of Figure 1. The amplitude of the bias at any given scale factor depends on the index n. The HI bias monotonically decreases with increasing scale factor for negative n. A negative value of n indicates that the HI density field was strongly biased in the past which decreases with time and eventually reaches unity at present. The decrease in bias corresponds to an overall dilution in the clustering of the HI mass distribution. The evolution of $\frac{S_c(a)}{S_c(a_i)}$ with scale factor for all these models is plotted in the top right panel of Figure 1.

The evolution of the configuration entropy is primarily governed by the growth of density perturbations which in turn is affected by the dynamics of the expansion of the Universe. Expansion of the Universe slows down the growth of perturbations. Besides the expansion, the time evolution of bias would also play an important role in controlling the dissipation of the configuration entropy of the Universe. For example, all the models with negative n show a decrease in the configuration entropy at earlier times. However, the dissipation slows down with time and in some cases it may even reverse its behavior and start to grow again with time. The time of reversal from dissipation to growth depends on the index n. A more negative index leads to an early reversal in the behavior of the configuration entropy.

The lower left panel of Figure 1 features the entropy rate as a function of scale factor in models with different n. The entropy rate is decided by the function $B(a) = b(a)D(a)\left[D(a)\frac{db(a)}{da} + b(a)\frac{f(a)D(a)}{a}\right]$ which consists of two terms and the combined contribution from these two

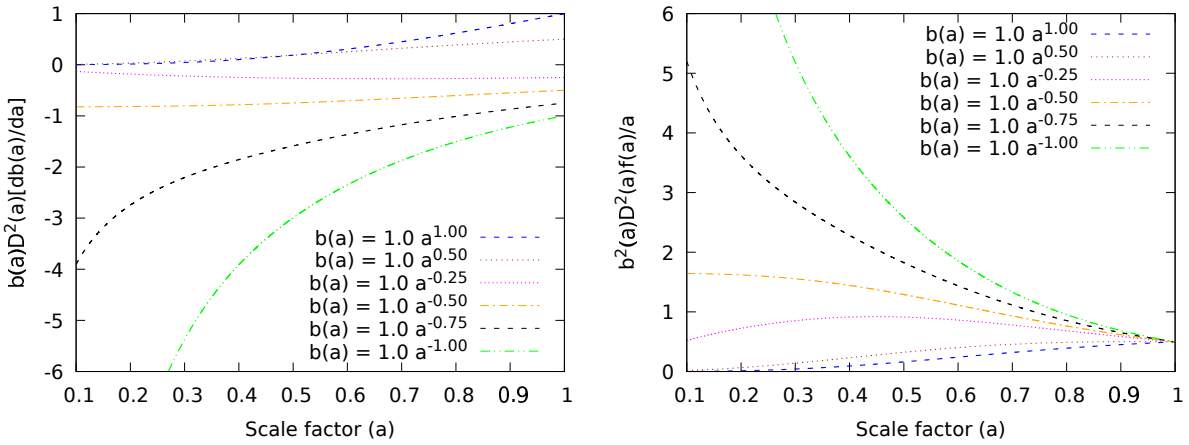

Fig. 2 The *left panel* displays the evolution of the first term in $B(a)$ with scale factor for models with different time evolution of bias. The *right panel* plots the evolution of the second term in $B(a)$ for the same models.

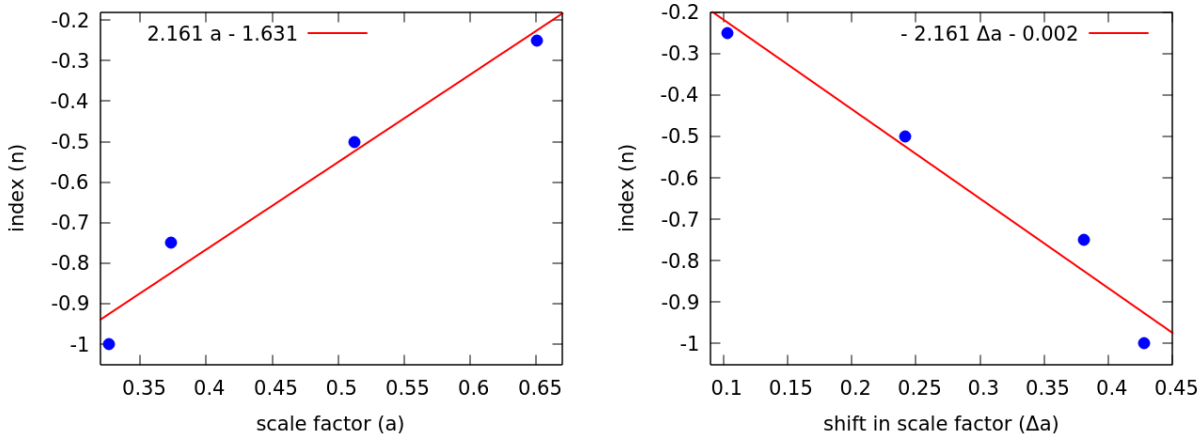

Fig. 3 The *left panel* displays the index (n) as a function of the location of the peaks in the derivative of entropy rate. The *right panel* plots the index (n) as a function of the shift of peak in the derivative of entropy rate with respect to unbiased ΛCDM model. We show together the best fit straight lines in both the panels.

terms decides the behavior of the entropy rate at any given time for any specific model. The two terms are separately plotted as a function of the scale factor for different models in the left and right panels of Figure 2. Clearly, a growth in entropy is expected when $B(a)$ is negative and a positive $B(a)$ is associated with entropy dissipation. For example, $B(a)$ is negative at all scale factors for $n = -1$ and this implies that there will be no dissipation of entropy in this model. On the other hand, the models with $n = 1$ and $n = 0.5$ have positive $B(a)$ at all scale factors and there is a continuous dissipation of entropy in these models. All the other models considered here show dissipation of entropy at some scale factors and growth of entropy at some other scale factors. A zero up crossing in the entropy rate corresponds to a local minimum in the configuration entropy. Clearly this zero up crossing appears at a smaller scale factor for more negative values of n.

We plot the derivative of the entropy rate in these models in the lower right panel of Figure 1. The derivative of the entropy rate exhibits a peak in all the models with negative n. We find that the location of the peak is sensitive to the index n and it appears at a smaller scale factor for models with smaller index. In an earlier work, Pandey & Das (2019) noted that in the unbiased ΛCDM model, this peak is located at the scale factor corresponding to the Λ-matter equality. We have used $\Omega_{m0} = 0.3$ and $\Omega_\Lambda = 0.7$ in the ΛCDM model. So in the unbiased ΛCDM model, the peak is expected to appear at $a = 0.754$. This can be clearly seen in the result depicted for the unbiased ΛCDM model in the same panel. Now the location of this peak is shifted towards a smaller scale factor when time evolution of bias is considered within the ΛCDM model. The shift is measured with reference to the location of the peak in the unbiased ΛCDM model. The magnitude of the entropy rate slows down after the

occurrence of this peak. In the unbiased ΛCDM model, the structure formation starts to slow down after the onset of Λ domination. The bias models with negative value of n dilute the clustering and slow down the structure formation even before the Λ-matter equality. This effect would manifest in a more prominent way in the models with more negative n. So, the peak in the derivative of the entropy rate is expected to exhibit a larger shift in these models. We measure the location of the peak in the models with different negative index and find them to be linearly related. The location and the shift of the peak are displayed as a function of the index in the left and right panels of Figure 3 respectively. The best fit relations between these parameters are also shown in the same figure.

We also consider two positive values of n in the time evolution of HI bias. A positive value of n indicates that the HI density field is anti-biased with respect to the underlying mass density field and the bias slowly increases from a very small positive value to unity at present. A decrease in anti-biasing with time would enhance the clustering of the HI leading to a continuous dissipation of the configuration entropy. In these models, entropy initially manifests a slower decrease than that of the ΛCDM model but then decreases quite quickly in the later part. We do not observe the peak in the derivative of the entropy rate in these models and they can be easily distinguished from the models with negative values of n. These models are not realistic and we consider them only for the sake of completeness.

In this work, we calculate the evolution of the configuration entropy of HI distribution in the post-reionization era assuming different time evolution of HI bias. We consider the flat ΛCDM model as the benchmark model of the Universe and within it consider the time evolution of HI bias as $b(a) = b_0 a^n$ with different values of the index n. We demonstrate that the time evolution of bias alters the position of the peak in the derivative of the entropy rate. The peak shifts towards a smaller scale factor for negative index and is absent when the index is positive. We find that the shift is linearly related with the index n and a larger shift is observed for a smaller index. We find the best fit relation between these two parameters and propose that identifying the location of this peak from observations would allow us to constrain the time evolution of bias within the framework of the ΛCDM model. We note here that the best fit line does not exactly pass through the points in each of the plots in Figure 3 even though the points we get are from theoretical calculations and hence exact. The reason for that is that the linear fit is used as a first approximation but it gives a pretty good fit. We also note that if any of the future surveys provides us with a suitable data set such that our method can be applied for analysis, there may be error bars which may be as big as the difference between the fit and the actual points. So, the linear approximation can work well in that situation.

One may consider some other quantity in the form $\int f(\rho_{\rm HI})dV$ and get another equation which might be utilized to constrain the HI bias function. The natural question that one can then ask is: why use configuration entropy? Part of the answer may be found in the Introduction where it was mentioned that this quantity has previously been used to study different cosmological problems. The Introduction also mentions that measurement of bias using configuration entropy is computationally advantageous compared to other methods. It has previously been shown that in a flat ΛCDM Universe with only matter and cosmological constant with scalar perturbation, the evolution of derivative of entropy rate with scale factor displays a distinct peak at a scale factor which is equal to the scale factor where matter-Λ equality occurs in that particular model. We calculate the shifts in the scale factor of the peak for a biased tracer from the scale factor of the peak for the unbiased case and find its correlation with the indices of the bias function. Since we are comparing the unbiased case with the biased case, we are compelled to use configuration entropy as the preferred quantity for analysis.

One can also measure the HI bias by comparing the two-point correlation function or power spectrum of the HI distribution with that for the underlying mass distribution. Combining these measurements at multiple redshifts would provide the time evolution of HI bias. However, such an analysis would require knowledge of the distributions of dark matter density field at different redshifts which can be obtained by employing N-body simulations. Contrary to this, the proposed method in this work does not require knowledge of the underlying mass density field at any redshift. The evolution of HI bias can be solely determined from the nature of evolution of the configuration entropy for the HI distribution. This is a remarkable advantage offered by the proposed method. It may be noted here that we do use the evolution of growing mode of dark matter to calculate entropy, but the evolution equation of growing mode is obtained under very general assumptions such as existence of scalar perturbation in an expanding Universe with presence of dark matter and cosmological constant with no interaction between dark matter and dark energy. Finally, we conclude that the method presented in this work provides an alternative method to constrain the evolution of HI bias using configuration entropy.

Acknowledgements The authors would like to thank an anonymous reviewer for useful comments and suggestions which have helped us improve the quality of the paper.

BP acknowledges financial support from the Science and Engineering Research Board (SERB), Department of Science & Technology (DST), Government of India through the project EMR/2015/001037. BP would also like to acknowledge IUCAA, Pune for providing support through the associateship programme.

References

Bagla, J. S., Khandai, N., & Datta, K. K. 2010, MNRAS, 407, 567
Bharadwaj, S., Nath, B. B., & Sethi, S. K. 2001, Journal of Astrophysics and Astronomy, 22, 21
Bharadwaj, S., & Sethi, S. K. 2001, Journal of Astrophysics and Astronomy, 22, 293
Bowman, J. D., Cairns, I., Kaplan, D. L., et al. 2013, PASA, 30, e031
Colless, M., Dalton, G., Maddox, S., et al. 2001, MNRAS, 328, 1039
Das, B., & Pandey, B. 2019, MNRAS, 482, 3219
Das, B., & Pandey, B. 2020, MNRAS, 492, 3928
Dekel, A., & Rees, M. J. 1987, Nature, 326, 455
Feldman, H. A., Frieman, J. A., Fry, J. N., & Scoccimarro, R. 2001, Phys. Rev. Lett., 86, 1434
Fry, J. N. 1996, ApJL, 461, L65
Gaztañaga, E., Norberg, P., Baugh, C. M., & Croton, D. J. 2005, MNRAS, 364, 620
Hamilton, A. J. S. 1992, ApJL, 385, L5
Hawkins, E., Maddox, S., Cole, S., et al. 2003, MNRAS, 346, 78
Huchra, J. P., Macri, L. M., Masters, K. L., et al. 2012, ApJS, 199, 26
Kaiser, N. 1984, ApJL, 284, L9
Kaiser, N. 1987, MNRAS, 227, 1
Lahav, O., Lilje, P. B., Primack, J. R., & Rees, M. J. 1991, MNRAS, 251, 128
Mann, R. G., Peacock, J. A., & Heavens, A. F. 1998, MNRAS, 293, 209
Martin, A. M., Giovanelli, R., Haynes, M. P., & Guzzo, L. 2012, ApJ, 750, 38
Masui, K. W., Switzer, E. R., Banavar, N., et al. 2013, ApJL, 763, L20
Mellema, G., Koopmans, L. V. E., Abdalla, F. A., et al. 2013, Experimental Astronomy, 36, 235
Norberg, P., Baugh, C. M., Hawkins, E., et al. 2001, MNRAS, 328, 64
Paciga, G., Albert, J. G., Bandura, K., et al. 2013, MNRAS, 433, 639
Padmanabhan, H., Choudhury, T. R., & Refregier, A. 2015, MNRAS, 447, 3745
Pandey, B., & Bharadwaj, S. 2007, MNRAS, 377, L15
Pandey, B. 2017a, MNRAS, 469, 1861
Pandey, B. 2017b, MNRAS, 471, L77
Pandey, B. 2019, MNRAS, 485, L73
Pandey, B., & Das, B. 2019, MNRAS, 485, L43
Peebles, P. J. E. 1980, The Large-scale Structure of the Universe (Princeton Univ. Press)
Sarkar, D., Bharadwaj, S., & Anathpindika, S. 2016, MNRAS, 460, 4310
Shannon, C. E. 1948, Bell System Technical Journal, 27, 623
Springel, V., White, S. D. M., Jenkins, A., et al. 2005, Nature, 435, 629
Switzer, E. R., Masui, K. W., Bandura, K., et al. 2013, MNRAS, 434, L46
Tegmark, M., & Peebles, P. J. E. 1998, ApJL, 500, L79
Tegmark, M., Blanton, M. R., Strauss, M. A., et al. 2004, ApJ, 606, 702
van Haarlem, M. P., Wise, M. W., Gunst, A. W., et al. 2013, A&A, 556, A2
Verde, L., Heavens, A. F., Percival, W. J., et al. 2002, MNRAS, 335, 432
Vogelsberger, M., Genel, S., Springel, V., et al. 2014, MNRAS, 444, 1518
York, D. G., Adelman, J., Anderson, John E., J., et al. 2000, AJ, 120, 1579
Zehavi, I., Zheng, Z., Weinberg, D. H., et al. 2011, ApJ, 736, 59
Zwaan, M. A., Meyer, M. J., Staveley-Smith, L., & Webster, R. L. 2005, MNRAS, 359, L30